



ORIGINAL ARTICLE

NLO potential exploration for D- π -A heterocyclic organic compounds by incorporation of various π -linkers and acceptor units



Muhammad Khalid ^{a,*}, Muhammad Usman Khan ^b, Iqra Shafiq ^a, Riaz Hussain ^b,
Khalid Mahmood ^c, Ajaz Hussain ^{c,*}, Rifat Jawaria ^a, Amjad Hussain ^b,
Muhammad Imran ^d, Mohammed A. Assiri ^{d,e}, Akbar Ali ^f,
Muhammad Fayyaz ur Rehman ^f, Keyu Sun ^g, Yuzhen Li ^{g,*}

^a Department of Chemistry, Khwaja Fareed University of Engineering & Information Technology, Rahim Yar Khan 64200, Pakistan

^b Department of Chemistry, University of Okara, Okara 56300, Pakistan

^c Institute of Chemical Sciences, Bahauddin Zakariya University, Multan 60800, Pakistan

^d Department of Chemistry, Faculty of Science, King Khalid University, P.O. Box 9004, Abha 61413, Saudi Arabia

^e Research Center for Advanced Materials Science (RCAMS), King Khalid University, P.O. Box 9004, Abha 61413, Saudi Arabia

^f Institute of Chemistry, University of Sargodha, Sargodha 40100, Pakistan

^g Department of Emergency, Minhang Hospital, Fudan University, No.170, Xinsong Road, Minhang District, Shanghai, 201199, China

Received 8 May 2021; accepted 24 June 2021

Available online 30 June 2021

KEYWORDS

Density functional theory (DFT);
 π -conjugated linkers;
NLO properties;
Structural modifications

Abstract Heterocyclic compounds with excellent nonlinear optical (NLO) properties are highly significant and have many potentials uses in various fields such as nuclear science, optoelectronics etc. Herein, an organic dye **JK-201** was used theoretically to design a series of novel D- π -A based NLO molecules (**DTA1-DTA12**). This novel series of NLO molecules was quantum chemically designed by structural tailoring at the 1st π -spacer and acceptors unit of the **JK-201** molecule. To explore the effect of spacers and acceptors on the electronic, photophysical, and NLO properties of **DTA1-DTA12**, density functional theory (DFT) investigations were performed for different simulation analyses. UV-Vis spectra revealed that all these novel compounds exhibited broader absorption spectra with the largest shift and a narrowed bandgap (1.84–2.07 eV) compared to the parent molecule (**JK-201**). Among all the designed compounds, the largest redshift was exam-

* Corresponding authors.

E-mail addresses: muhammad.khalid@kfueit.edu.pk, Khalid@iq.usp.br (M. Khalid), ajaz_hussain01@yahoo.com, drajazhussain@bzu.edu.pk (A. Hussain), fayyaz9@gmail.com (M.F. ur Rehman), liyuzhenmhh@126.com (Y. Li).

Peer review under responsibility of King Saud University.



Production and hosting by Elsevier

ined in **DTA11** (538.99 nm). Furthermore, with the help of frontier molecular orbital (FMO) study, charge transfer processes between the orbitals and chemical reactivity of designed molecules were explained. Moreover, the Energy gap ($E_{\text{LUMO}}-E_{\text{HOMO}}$) was also used to express global reactivity parameters (GRPs). These GRP findings evaluated that all molecules (**DTA1-DTA12**) had higher global softness ($\sigma = 13.15-14.77$ a.u) and lower hardness ($\eta = 0.034-0.038$ a.u) values, which indicated that these compounds were more reactive. Nevertheless, significantly higher NLO behavior was examined in all compounds. Overall, compound **DTA5** showed a larger value of the linear polarizability ($\langle \alpha \rangle = 2868.08$ a.u.), while compound **DTA12** displayed a larger hyperpolarizability ($\beta_{\text{total}} = 268494.71$ a.u) value. This present work presented that by controlling the type of π -spacer and acceptor units, metal-free NLO materials can be designed, which can be valuable for hi-tech NLO applications.

© 2021 The Authors. Published by Elsevier B.V. on behalf of King Saud University. This is an open access article under the CC BY license (<http://creativecommons.org/licenses/by/4.0/>).

1. Introduction

Second-order nonlinear optics (NLO) is a significant branch of science that started with the discovery of second harmonic generation (SHG) and considered as a fundamental process for optical frequency conversion in quantum and classical optics (Iliopoulos et al., 2010; Kilper, 2010; Manzoni et al., 2015). In second-order NLO, lasers having a high degree of directionality, coherence and spectral purity are used to irradiate the atoms and molecules with their interatomic field comparable electric field. Laser-matter interactions are fundamentally understood in the second-order NLO process, which leads to the NLO effects implementation in different technological areas, including optical data storage, optical switching and optical communication (Lacroix et al., 1994; Manzoni et al., 2015; Wu et al., 2012). Therefore, designing and synthesis of NLO materials is an important area of research for decades. Second-order NLO materials have a promising role in different fields, including atomic, molecular, solid-state physics, chemical dynamics, medicine, surface interface sciences, biophysics and materials science (Eaton, 1991; Zyss and Ledoux, 1994). Moreover, they are also gaining remarkable importance in electro-optics-based signal-analysis, fiber optics, telecommunications and information technology (Breitung et al., 2000; Kasap and Capper, 2017; Peng and Yu, 1994; Tsutsumi et al., 1998). Therefore, different efforts are made in modelling various materials such as inorganic and organic semiconductors, natural and synthetic nanomaterials, molecular dyes and polymer systems that show NLO properties (Anthony et al., 2008; Ivanov et al., 2013; Khoo, 2014; Yamashita, 2011). The organic complexes are considered better options in NLO materials due to their effortless reaction chemistry, cheap development, and structural modifications, which help us change them chemically for a unique NLO response.

Centric compounds with delocalized π -electrons framework adequately participate with substituted donors and acceptor moieties. Over the past several years, a significant number of metal-free organic donor-acceptor complexes have been identified as NLO compounds with π -conjugated linkers that offer a path for the charge transfer of electron in the presence of an electric field (Janjua, 2012; Janjua et al., 2014a; Janjua et al., 2015b; Janjua et al., 2014b). However, the tunable absorbance wavelength and quick skeleton modification

using unique substituents, allowing researchers to model the chemical structure for excellent NLO response (Hochberg et al., 2006; Kulyk et al., 2017; Spiridon et al., 2015; Sung and Hsu, 1998). The use of intramolecular charge transfer (ICT) between electron donor and withdrawal group to build a new π -donor-acceptor system can minimize the bandgap and also regulate the transitions utilizing various donor or acceptor moieties with larger second-order NLO or first hyperpolarizability values (β) (Janjua, 2012; Janjua et al., 2014a; Janjua et al., 2015b; Janjua et al., 2014b; Janjua et al., 2016).

The synthesis and electronic properties of system (D- π -A) units with the new π -conjugated system is introduced in our system consisting of four π -spacers 5,6-difluorobenzo[c] (Eaton, 1991; Peng and Yu, 1994) thiophene[3,2-b] thiophen-2-yl)-1,1,4,4,4-hexafluorobut-2-ene-2 sulfonic acid, thiophene benzo[c] and thiazole were used as first π -linker. Triphenylamine (TPA) and acceptor Thienothiophene (TTS) TPA, a donor unit due to its capacity for electron donation and charge transfer, are used in many hole transport materials (Long et al., 2014; Roncali, 2009). Moreover, an excellent linkage between D and A units could be facilitated by π -linkers whose huge diversification is present in the literature. Push-pull architecture has been built by designing D- π -A organic molecules through assimilation of suitable D, π -bridge, and A units. So, pull-push arrangements accommodate to decrease charge recombination, influence charge separation, deepen the absorption range toward longer wavelength, magnify asymmetric electronic distribution, decrease HOMO-LUMO bandgap hence elevated NLO response (Haroon et al., 2017; Janjua, 2012; Janjua et al., 2015a; Janjua et al., 2010).

In the current investigation, we design a number of new (D- π -A) molecules (**DTA1-DTA12**) by the modification of first π -spacers and acceptors by using a reference compound **JK201** (Khan et al., 2019a; Paek et al., 2010). Based on NLO properties, we study the efficacy of investigated compounds as effective NLO compounds. The literature data reveals that the NLO properties of designed compounds (**DTA1-DTA12**) have not been published yet. To fulfill this research gap, DFT calculations for electronic characteristics, absorption spectrum, polarizability and first hyper-polarizability values were performed to compute the newly designed dyes. Hopefully, this research will act as a means to create new metal-free organic dyes with tremendous NLO properties.

2. Computational procedure

This present investigation was accomplished to probe the NLO behavior of newly designed molecules (**DTA1-DTA12**). Density functional theory/time dependent-density functional theory (DFT/TD-DFT) computations were used to determine electronic structures, NLO properties and absorption spectra (UV-Vis analysis) of **DTA1-DTA12**. Gaussian 09 program package (Frisch et al., 2009a) was employed to perform all computations. By utilizing the B3LYP level of theory and 6-31G(d,p) basis set, geometrical optimization of all the species was executed in the gaseous phase (Ali et al., 2020; Khalid et al., 2020c). The absence of negative frequency confirmed the stability of optimized geometries. These optimized geometries are then further used to understand the determination of energy gaps between HOMO and LUMO (FMO analysis), linear polarizability $\langle \alpha \rangle$ and hyperpolarizability (β_{total}) investigation at aforesaid functional and basis set by DFT. Following equations were utilized for calculating the $\langle \alpha \rangle$ and (β_{total}).

$$\langle \alpha \rangle = 1/3(\alpha_{xx} + \alpha_{yy} + \alpha_{zz}) \quad (1)$$

$$\beta_{total} = [(\beta_{xxx} + \beta_{yyy} + \beta_{zzz})^2 + (\beta_{yyy} + \beta_{zzz} + \beta_{yxx})^2 + (\beta_{zzz} + \beta_{xxx} + \beta_{zyz})^2]^{1/2} \quad (2)$$

Total ten hyperpolarizability tensors, β_{xxx} , β_{xyy} , β_{xzz} , β_{yyy} , β_{xxy} , β_{yzz} , β_{zzz} , β_{xxz} , β_{yyz} and β_{xyz} were achieved as an output from Gaussian file in x, y and z directions. To determine the absorption spectra, a high functional method was crucial for D- π -A-type molecules. Therefore, transition energies were accomplished by TD-DFT utilizing a corrected version with improved properties of B3LYP, hybrid exchange-correlation functional using the coulomb-attenuating method (CAM-B3LYP) along with 6-31G(d,p) (Yanai et al., 2004). Some software Avogadro (Hanwell et al., 2012), GaussView 5.0 (Frisch et al., 2009b) and Chem-Craft (Zhurko and Zhurko, 2009) were utilized to calculate the results.

3. Results and discussion

This current quantum chemical investigation illustrated the theoretical design and explored the innovative organic NLO chromophores. In order to modulate the magnificent NLO compounds, an organic metal-free synthesized dye named **JK-201** was used, which exhibited appealing NLO properties (Khan et al., 2019a). Structurally, **JK-201** was composed of three parts: N-(9,9-dimethyl-9H-fluoren-3-yl)-9,9-dimethyl-N-phenyl-9H-fluoren-2-amine (**DMFA**) as a donor moiety, 5-methyl-2,3-dihydrothieno[3,4-b][1,4]dioxine (**EDOT**) and 2,5-dimethylthieno[3,2-b]thiophene (**TTPH**) as 1st and 2nd π -spacer, respectively, that collectively formed π -conjugated bridge and end capped acceptor 2-cyanoacrylic acid (**CAA**) as an acceptor moiety (Fig. 1a). Literature studies revealed that for the fine-tuning of interchange transfer properties, HOMO/LUMO band gap and absorption spectrum, π linkers and A moiety played significant roles (Khan et al., 2018). Therefore, we designed an innovative series of metal-free dyes (**DTA1-DTA12**) by modulating the 1st π -spacer and acceptor unit while keeping the D moiety and 2nd π -spacer preserve, with the motivation to gain excellent NLO materials

(Figs. 1a and 1b). In the first four compounds, **DTA1** to **DTA4** first π -linker (**EDOT**) was modulated with **FMB**, **DMT**, **FMC** and **DPT**, which possessed more electron richness and preferable planarity (Khan et al., 2019a) while **CAA** is replaced with **FBSA**. Similarly, compounds **DTA5** to **DTA8** were tailored by using spacers mentioned above along with **ETAA** more powerful acceptor unit. Likewise, molecules **DTA9** to **DTA12** were obtained by tailoring the A unit with **ETMN** accompanying the above-mentioned π -linker units. The pictographs of these dyes were displayed in Figs. 2a and 2b. To evaluate how various π -spacers and acceptor units influenced the NLO properties such as hyperpolarizability (β_{total}), polarizability $\langle \alpha \rangle$, absorption spectrum and electronic properties, DFT/TD-DFT study was carried out in **DTA1** to **DTA12**.

3.1. Frontier molecular orbital (FMO) analysis

To explain the reactivity, possibility of charge transfer and potential for the light absorption of the molecules, FMO investigation is a remarkable tool (Peng and Yu, 1994). These factors are directly related to the bandgap of HOMO/LUMO orbitals. Herein, HOMO is regarded as an electron donor, which is the highest electronically filled molecular orbital, while LUMO is generally attributed as an acceptor and is empty or unfilled orbital (Chemla, 2012). Molecules with smaller HOMO-LUMO distance are regarded as more reactive, less stable as well as soft compounds. Such molecules exhibited larger possibilities for the intramolecular charge transfer (ICT); hence, more polarized so, will serve as a finer competitor in offering the best NLO response (Dai et al., 2018; Ferdowsi et al., 2018b; Nagarajan et al., 2017; Yamada et al., 2018). In this consideration, energies of HOMO/LUMO, HOMO-1/LUMO + 1 and HOMO-2/LUMO + 2 of **DTA1-DTA12** were calculated, and results were tabulated in Tables S13 (a) and S13 (b).

Fig. 3 represented that all the derivatives shown lower HOMO/LUMO energies with smaller bandgap than reference chromophore except **DTA6**, which expressed HOMO-LUMO energies comparable to reference. Further, Table S13 (a) elucidated that the HOMO/LUMO and bandgap energy (2.13 eV) of the reference compound (**JK201**) was higher (Khan et al., 2019a) than all its derivatives (**DTA1-DTA12**). The Eg values of all the designed dyes were decreasing gradually from 2.07 to 1.84 eV. Among **DTA1** to **DTA4** compounds with **FBSA** as end capped acceptor moiety, the largest Eg value (2.00 eV) was calculated in **DTA2**, in which **DMT** was used as the first π -linker. This Eg was reduced to 1.98 eV in **DTA4**, then diminished to 1.97 eV in **DTA3** and further becomes lessen to 1.88 eV in **DTA1** as the first π -spacer changes **DPT**, **FMC** and **FMB**, respectively. The same phenomena was investigated among the **ETAA** acceptor unit family (**DTA5** to **DTA8**), the compound **DTA6** with **DMT** first π -linker exhibited the huge Eg (2.07 eV). In comparison, the least value was found in **DTA5** (1.93 eV), in which **FMB** was used as the first π -bridge. Similarly, **DTA9** - **DTA12** compounds with **ETMN** acceptor decreased in Eg and were observed as **DTA10** > **DTA11** > **DTA12** > **DTA9** as their first π -linker changes. Nevertheless, it was also examined that

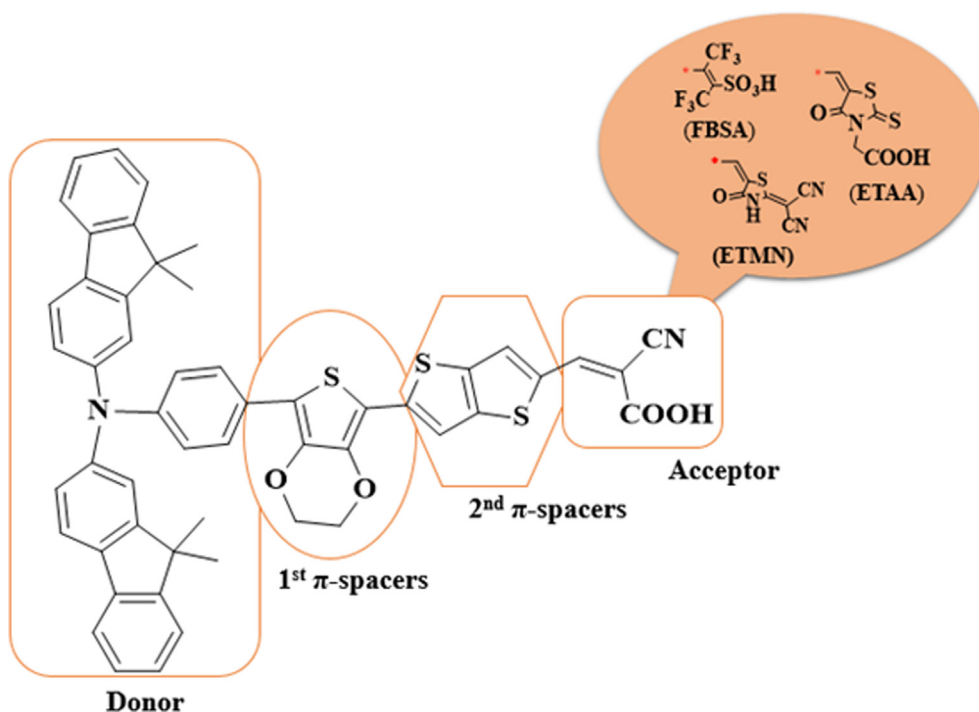


Fig. 1a Sketch map of reference molecule (JK-201) and various acceptors used in the designed compounds.

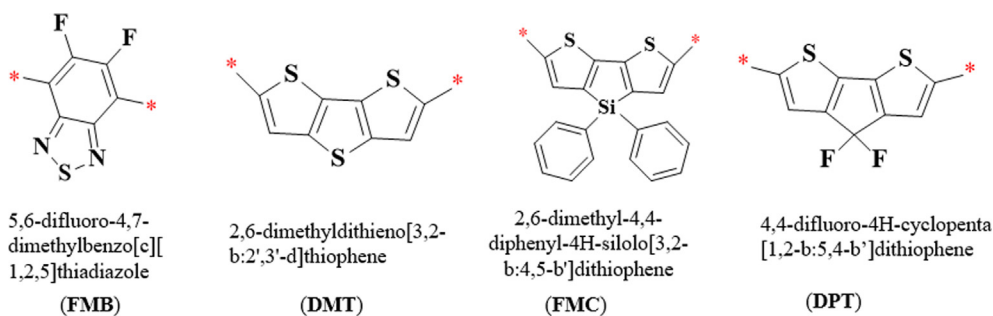


Fig. 1b The different 1st pi-spacer structures used in the designed compounds.

the compounds with FMB as the first π -linker exhibited low bandgap.

On the other hand, **DMT** first π -spacer species showed a larger HOMO/LUMO energy difference. Among all the designed dyes, in compound **DTA9**, the least E_g was studied. The combined effect of electron-rich and planar π -linker FMB (5,6-difluoro-4,7-dimethylbenzo[c]thiadiazole) (Eaton, 1991; Peng and Yu, 1994) and powerful acceptor moiety ETMN(2-(5-methylene-4-oxothiazolidin-2-ylidene)malononitrile), collectively reduced the distance between HOMO and LUMO (1.84 eV) in **DTA9** than from its reference dye (2.13 eV). Overall, calculated E_g of the organic dyes **DTA1-DTA12** was increased in the following order: **DTA9** < **DTA12** < **DTA11** < **DTA1** < **DTA10** < **DTA5** < **DTA3** < **DTA4** < **DTA7** < **DTA2** < **DTA8** < **DTA6**.

Along with the magnitude of the energy gap of orbitals, the capability of species to undergo ICT towards acceptor from the donor through π -spacers is also a significant aspect for NLO structure–function relationships (Khalid et al., 2020a). Surfaces of FMOs were utilized to reveal the transfer of

charges, as displayed in Fig. 4 and Fig. S1. In all designed dyes, the HOMO was predominantly located over the donor DMFA part and partially on the π -bridge. LUMO charge density was mainly presented over the terminal acceptor units and partly over the π -spacers (Fig. 4). Similarly, for HOMO-1, the electronic cloud is located majorly over the π -bridge and acceptor units and minorly over the donor part, while for LUMO, it is concentrated over the acceptor and π -spacers (see Fig. S1).

This facilitation indicated the efficient charge transfer by π -conjugates from the D moiety towards A unit ensures that all the analyzed dyes (**DTA1-DTA12**) would be significant NLO materials.

3.2. Global reactivity parameters

The E_g ($E_{\text{LUMO}} - E_{\text{HOMO}}$) is the most significant factor for the evaluation of the global reactivity parameters (GRPs) such as global hardness (η), global softness (σ), global electrophilicity index (ω) electron affinity (EA), ionization potential (IP) (Fukui, 1982) electronegativity (X) and chemical potential (μ)

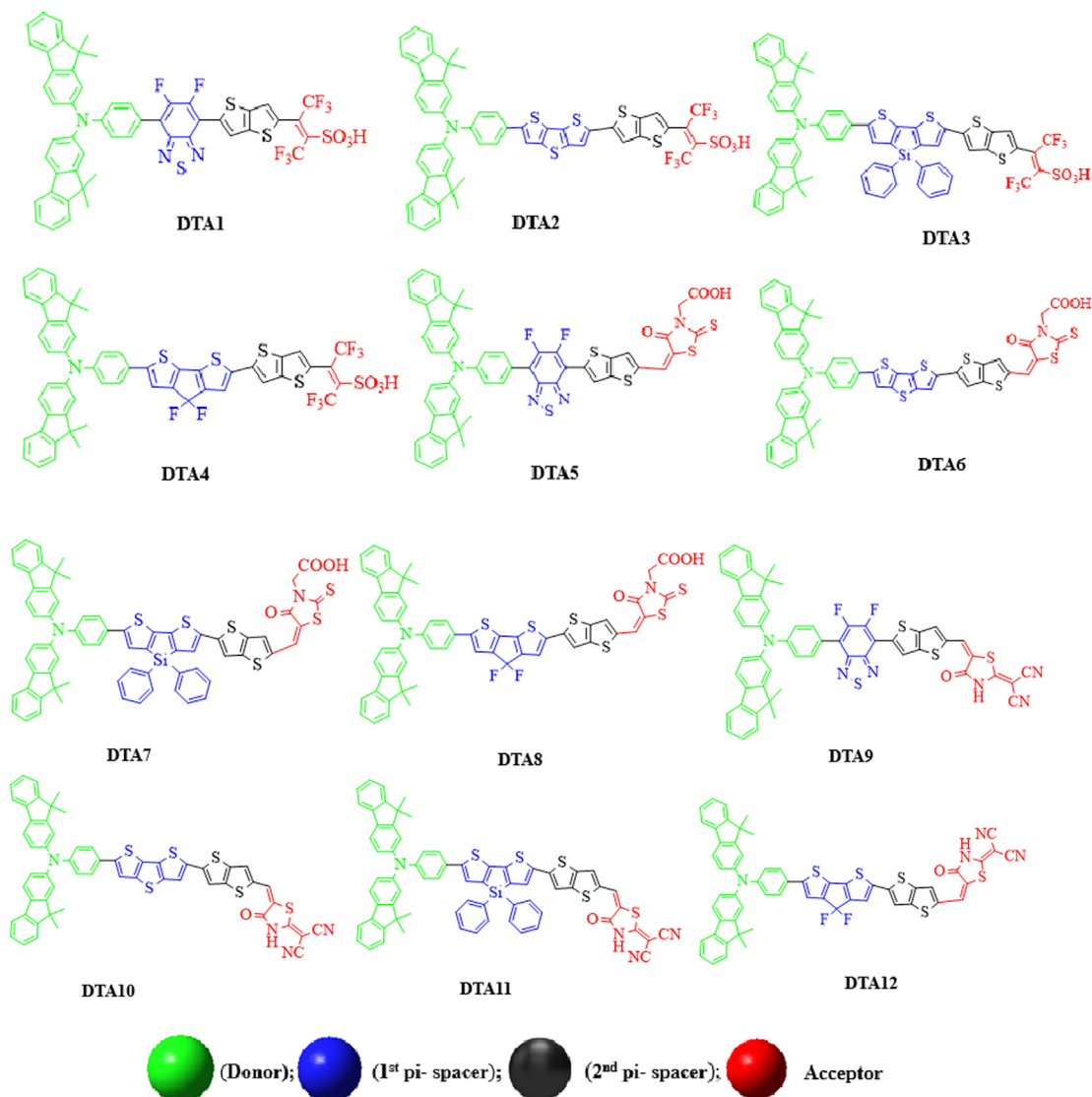


Fig. 2a Structures of designed dyes (DTA1-DTA12).

(Chattaraj et al., 2006; Lesar and Milošev, 2009; Parr et al., 1978; Parr et al., 1999). The energy necessary to extract the electron from the HOMO orbital is equal to the ionization potential, which expressed the electron-donating and electron-accepting ability of an atom. This parameter is used to measure the electrophilic strength of compounds. Furthermore, the HOMO/LUMO energy gap was directly related to chemical potential, hardness, and compound stability while inversely associated with reactivity. Therefore, molecules with smaller E_g were regarded as more reactive, less stable and soft molecules considered far more polarized and serve as a finer competitor in offering the best NLO response (Dai et al., 2018; Ferdowsi et al., 2018a; Khalid et al., 2020a). Thus, global reactivity parameters are appealing to researchers to conduct large-scale analysis. The calculated GRP of investigated compounds are shown in Table 1.

Above table elucidated that reference chromophore have the greater value of hardness ($\eta = 0.039$ a.u.) as well as chemical potential ($\mu = -0.140$ a.u.) while greater values for global softness ($\sigma = 12.775$ a.u.) than all its derivatives. These GRP

results indicated that **JK-201** is more stable and less reactive, hence showed lower NLO response as compared to its derivatives. Interestingly all the designed dyes expressed least values of hardness ($\eta = 0.034$ – 0.038 a.u.) as well as chemical potential ($\mu = -0.151$ to -0.139 a.u.) while greater values for global softness ($\sigma = 13.15$ – 14.77 a.u.). Among designed compounds, **DTA9** exhibited higher value of softness (14.778 a.u.) so, it shows highest reactivity. The decreasing order of softness; **DTA9** > **DTA12** > **DTA11** > **DTA1** > **DTA10** > **DTA5** > **DTA3** > **DTA4** > **DTA2** > **DTA8** > **DTA6**. > **JK-201**. Hence, all the molecules exhibited higher value of softness which indicated more reactivity as well polarizability resulting excellent NLO response.

3.3. UV-Vis spectra

Employing TD-DFT computation, absorption spectra of the designed compounds have been calculated to understand the effect of bridging core moieties and acceptor units on spectral properties. The calculated results of absorption wavelength

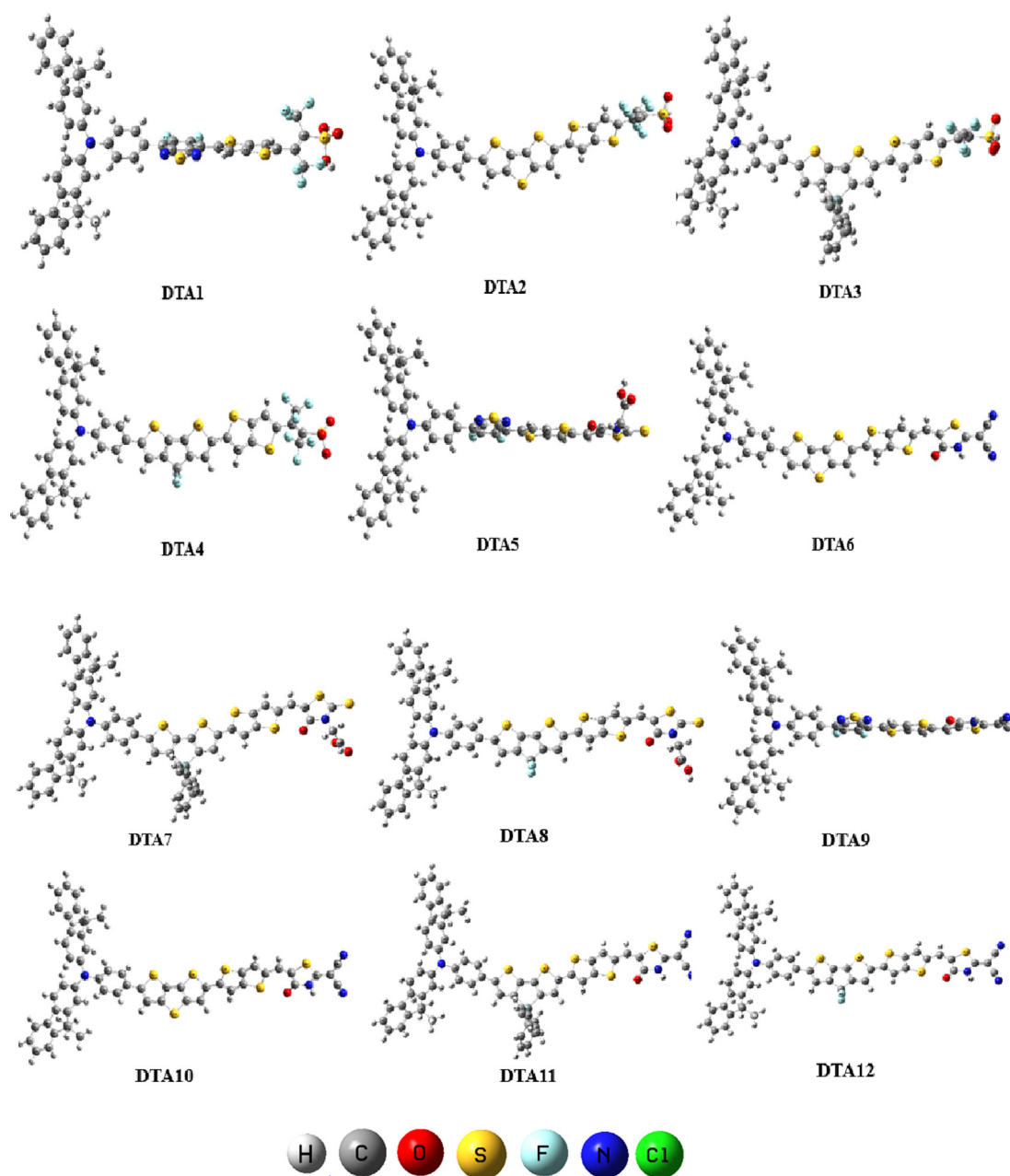


Fig. 2b Optimized geometries of investigated compounds (DTA1 – DTA12) at B3LYP/6-31G(d,p) level of theory.

(λ_{max}), transition energy (E_{ge}), transition moment (M_{λ}^{gm}), oscillator strength (f_{os}), transitions nature and light-harvesting efficiency (LHE) of the designed compounds (DTA1-DTA12) were presented in Tables 2.

Table 2 elucidated a significantly close relationship was presented between experimental and theoretical value, which supported the selected methodology for DFT analysis was appropriate enough. Interestingly, all the designed compound (DTA1-DTA12) exhibited a larger value of λ_{max} than their reference molecule (JK-201) 484.7 nm (Khan et al., 2019a) except DTA2 and showed absorbance spectra in the visible region as shown in the spectrum (Fig. 5). It was seen that λ_{max} values are greatly influenced by preferable planarity and more electron richness π -spacer and end-capped electron acceptor motifs, which in turn push the absorption spectra towards redshift

(Ans et al., 2019; Khalid et al., 2020b; Paek et al., 2010). So, DTA2 exhibited lower absorption properties due to the poor electron-withdrawing nature of DMT as no electronegative atom was presented in its structure compared to other π -spacers (Figs. 1a and 1b). The simulated spectra of designed compounds existed between 462.5 and 539 nm. Among all entitled molecules, the larger computed λ_{max} finding was found in the compounds (DTA11, DTA7 and DTA3) having FMC as first π -spacer (Table 2) as FMC π spacer enhances the conjugation hence, stabilized the molecule which in result showed redshift. Furthermore, molecules (DTA2, DTA6 and DTA10) with DMT π spacer exhibited the least value of λ_{max} with the same acceptor units. Additionally, it was also analyzed that the dyes with ETMN acceptor units were red-shifted while FBSA acceptor unit containing molecules exhibited blue shift

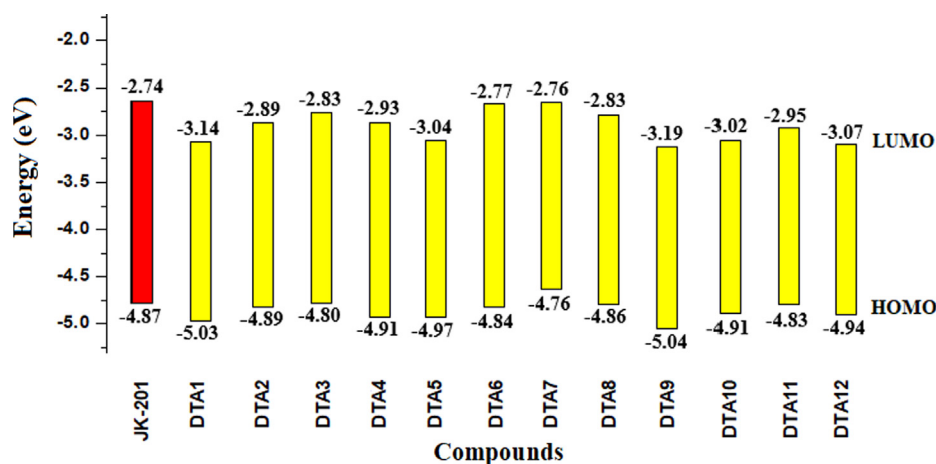


Fig. 3 Graphical representation of HOMO/LUMO energies of entitled chromophores.

(Table 2). The ETMN acceptor had a cyclic structure with a more powerful electron-withdrawing cyano ($-\text{CN}$) group. Resonance due to a five-member ring and strong electron-withdrawing $-\text{CN}$ group (Ali, 2021) enhanced the stability by lowering the E_g value and show maximum absorption properties as compared to FBSA, which contain fewer electron-withdrawing (CF_3 , SO_3H) groups as compared to cyano. The reducing order for λ_{max} of the designed compounds is: **DTA11** > **DTA12** > **DTA7** > **DTA8** > **DTA9** > **DTA5** > **DTA10** > **DTA6** > **DTA3** > **DTA4** > **DTA1** > **DTA2**. Transitions in the **DTA1-DTA12** were arisen from HOMO to LUMO, which was according to the principle of most donor- π -acceptor organic molecules. Chief donation in these excitations belongs to the HOMO \rightarrow LUMO (31–52%) and HOMO-1 \rightarrow LUMO supply (31–51%). So, it was cleared that by the structural modelling of the parent compound (JK-201) in 1st π -spacer and acceptor parts, λ_{max} can be enhanced in derivatives which would be appealing NLO novel dyes.

LHE is a significant component that expresses the optical efficiency of the designed compounds, which can be obtained by using f_{os} , provided by the TD-DFT computations. It is considered that the more excellent photocurrent response is investigated by the compound, which has greater LHE. Using Eq. (3), the LHE of the designed dyes was calculated (Xie, 2001) and results were displayed in Table 2.

$$LHE = 1 - 10^{-f} \quad (3)$$

Oudar and Chemla formulated a two-state model (Oudar and Chemla, 1977) extensively utilized in the literature to analyze NLO response containing the critical excited and ground state e in sum-over-state expression. In this model, an interaction was formed between the charge transfer transition and 2nd order polarizability, the origin of push-pull architecture for modelling remarkable NLO compounds.

$$\beta_{\text{CT}} = \frac{\Delta\mu_{\text{gm}}f_{\text{gm}}}{E_{\text{gm}}^3} \quad (4)$$

Eq. (4) showed two-state model expression, where (β_{CT}) first hyperpolarizability, ($\Delta\mu_{\text{gm}}$) dipole moment difference, (f_{gm}) oscillator strength and (E_{gm}^3) cube of transition energy among ground and m th excited state. Eq. (4) revealed that

β_{CT} directly relates to the product of $\Delta\mu_{\text{gm}}$ and f_{gm} and inversely related with the transition energy.

So, the molecules with optimum NLO behavior had a larger magnitude of $\Delta\mu_{\text{gm}}$ and f_{gm} and smaller E_{gm}^3 . Herein, $\Delta\mu_{\text{gm}}$, f_{gm} , and E_{gm}^3 were calculated from spectral analysis, and results were shown in Table 3. The results indicated that among derivatives, the higher value for E_{gm}^3 **DTA3** (2.7 eV) was found, while a smaller value was exhibited in **DTA12** (2.3 eV). Moreover, to further enhance the NLO finding, the relationship between the two-state model (β_{CT}) and β_{total} values for all dyes (**DTA1-DTA12**) is displayed in Fig. 6. The rise and fall in the graph indicate the effect of different π -spacer and terminal acceptor units on β_{total} values related to the rise and fall predicted by two-level model (β_{CT}) results. It is evident from Fig. 6 that the β_{total} values of studied compounds **DTA1**, **DTA5**, **DTA6**, **DTA7**, **DTA8**, **DTA10** and **DTA11** are in broad agreement with two-state model (β_{CT}) results which support our claim of their potential to be used as efficient NLO compounds.

3.4. Nonlinear optical (NLO) properties

In optoelectronic devices, telecommunication, networking and signal manipulation, NLO products are extensively utilized. The optical behavior depends upon the electrical properties of the entire molecule, which are successively related to the linear ($\langle\alpha\rangle$) and nonlinear (β_{total}) responses. Furthermore, it will be entrancing to see how these NLO properties vary with modifying π -linkers and acceptor units. Herein, NLO responses of entitled dyes (**DTA1-DTA12**) were estimated, and results were displayed in Tables 2 and 3.

Table 3 revealed that the linear polarizability ($\langle\alpha\rangle$) values of the parent compound are lesser (914.08 a.u.) (Khan et al., 2019a) than its derivatives (**DTA1-DTA12**). Among all the designed molecules, the species with FMC as 1st π -spacer **DTA3** and **DTA11** exhibited a huge value of $\langle\alpha\rangle$ 1183.91, 2868.08 and 1391.12 a.u., respectively while FMB containing molecules expressed the least values except **DTA5** in the ETAA family (Table 3). Overall, the investigation revealed that dyes with ETMN acceptor unit (**DTA9-DTA12**) manifested an enormous value of $\langle\alpha\rangle$. However, compounds structurally

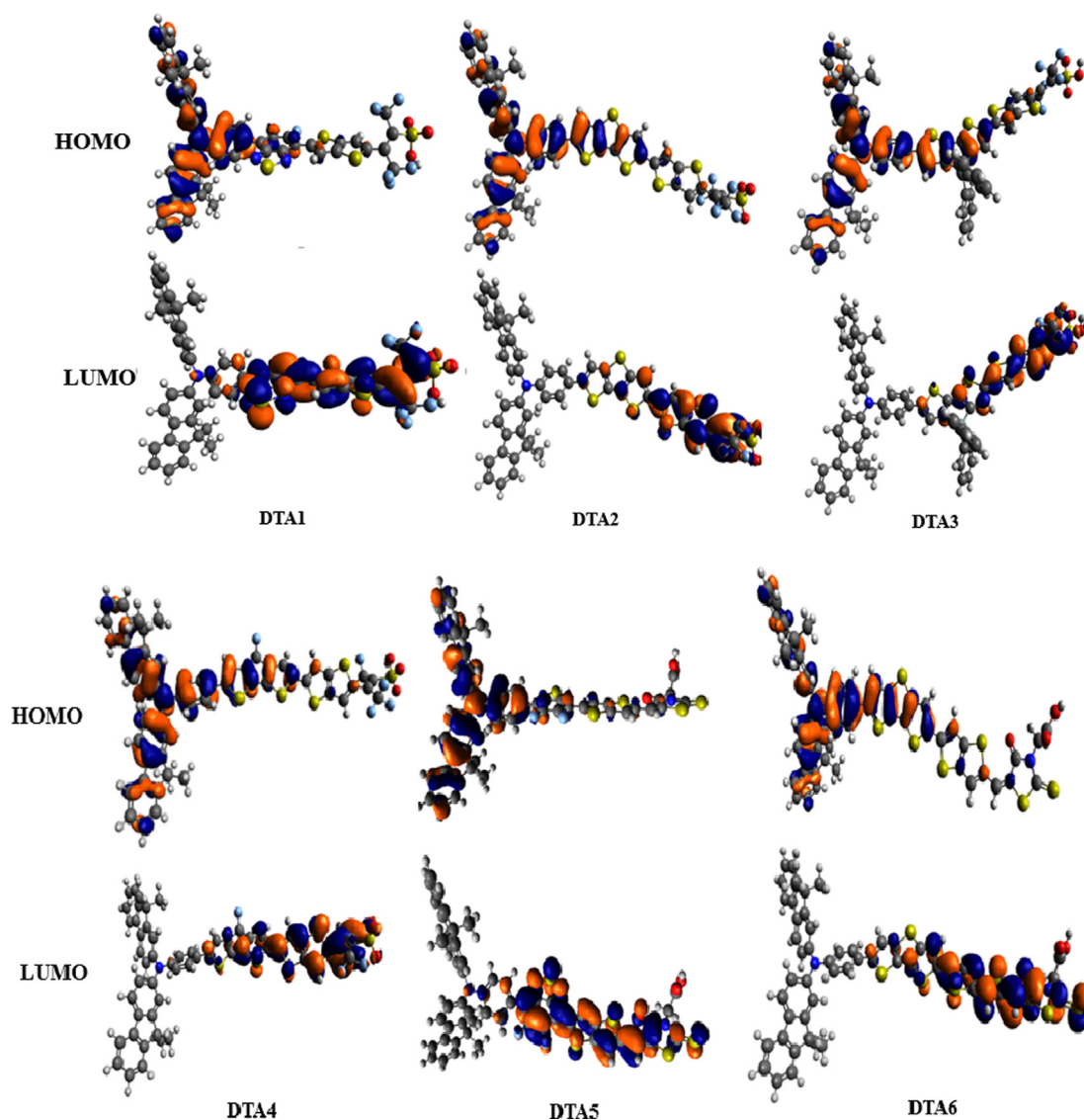


Fig. 4 The contour of HOMO and LUMO orbitals of the studied dyes.

tailored with FBSA acceptor moiety (DTA1-DTA4) have the least linear polarizability values with the same π linkers. Among all the dyes, the greater value was investigated in DTA5 (2868.08 *a.u.*), and compound DTA1 exploited a smaller value (939.89 *a.u.*) for linear polarizability. Nevertheless, average polarization of all the explored dyes increases in the following order: DTA5 > DTA11 > DTA7 > DTA12 > DTA10 > DTA8 > DTA3 > DTA6 > DTA9 > DTA4 > DTA2 > DTA1.

The literature study disclosed that average polarizability was affected by energy gap values. It was evident that a smaller bandgap and larger linear polarizability designated greater hyperpolarizability, referring to the large NLO values (Mohankumar et al., 2015; Qin and Clark, 2007). Equation (5) illustrates the calculation of dipole polarizability (along the x-axis):

$$\alpha \propto \frac{(M_X^{\text{gm}})^2}{E_{\text{gm}}} \quad (5)$$

Herein, M_X^{gm} represents the transition moment, and E_{gm} refers to the transition energy between ground $\rightarrow n_{\text{th}}$ excited state. A direct relationship exists between $\langle \alpha \rangle$ and M_X^{gm} whereas an inverse relation is seen with the E_{gm} . The transition dipole moment demonstrates the electronic transition effects and interactions of dyes with certain electromagnetic waves of the given polarization. Generally, it was investigated that a molecule with higher M_X^{gm} value and minor E_{gm} value presented greater hyperpolarizability values (Khan et al., 2019b). Therefore, for the assessment of attractive NLO properties of species, dipole polarizabilities were found as a quantitative estimation. As the first hyperpolarizability endorsed the estimation of NLO behavior of compounds which was successively related with the intermolecular charge transfer (ICT) towards A unit from D moiety *via* π -linkers. Such interaction was studied in our designed compounds, as displayed in Fig. 3. Electron density interacts with the external field, which enhanced the dipole moment, leading to higher first-order

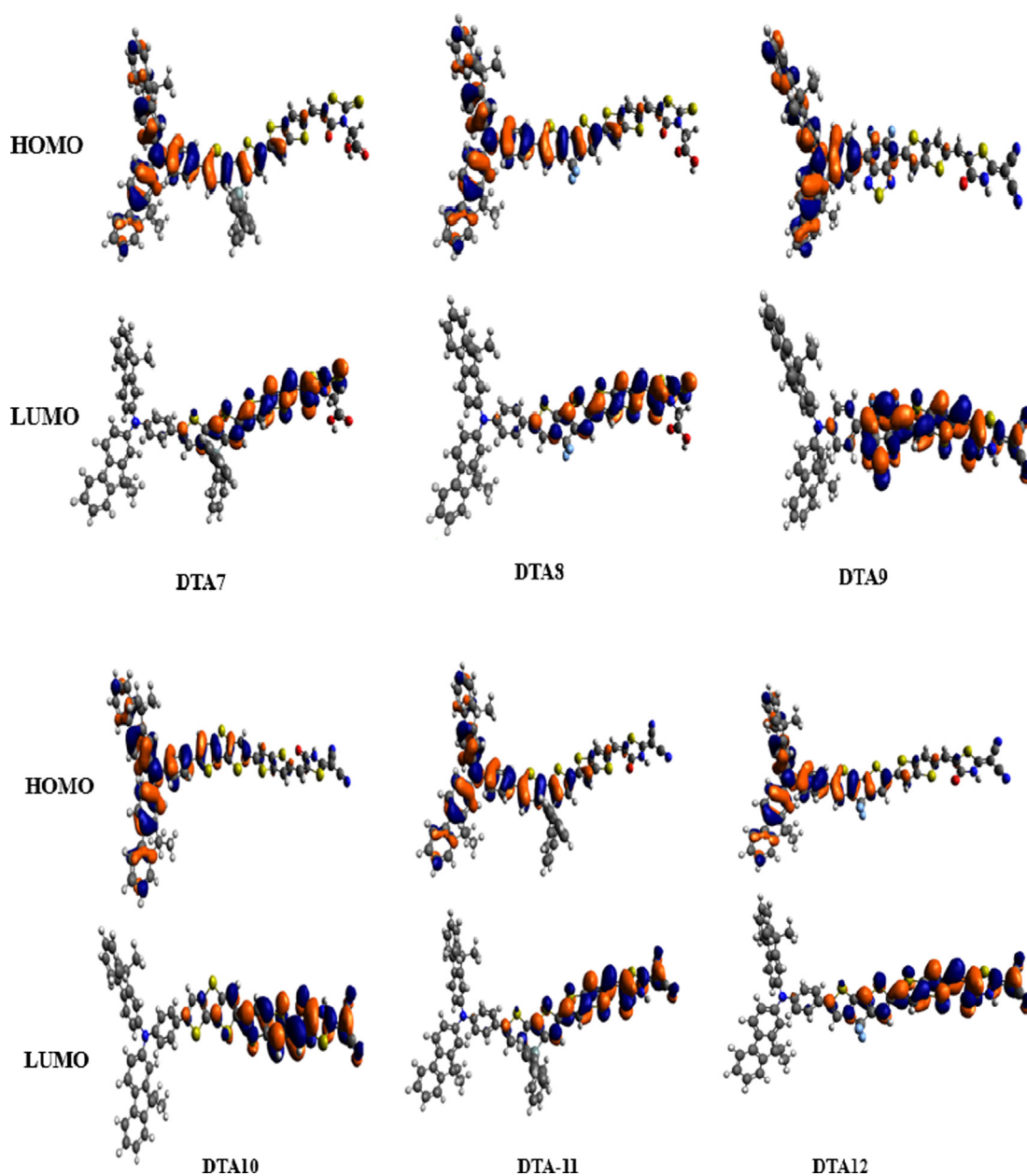


Fig. 4 (continued)

hyperpolarizability. The calculated results of second-order polarizability of entitled dyes were explored in Table S14 while their graphical representation is done in Fig. 7.

These DFT investigations explained that the calculated 2nd order polarizability (β_{total}) for all the designed dyes (DTA1-DTA12) were more significant than that of their parent compound (JK-201), 104093.90 *a.u.* (Khan et al., 2019a). Fig. 7 explored that the chromophores with ETMN acceptor moiety and DPT spacer expressed remarkable β_{total} values than other acceptors and spacers units. Further, among FBSA, ETAA and ETMN terminal acceptor unit families, compounds with DPT 1st π -spacer DTA4, DTA8 and DTA12 expressed larger hyperpolarizability 174280.17, 188317.42 and 268494.70 *a.u.*, respectively. Furthermore, these values decrease as the 1st π -spacer DPT is replaced with FMC.DMT and FMB, respec-

tively. Moreover, it was also examined that dyes with FMB π -bridge manifested the least values except in the FBSA acceptor unit family, in which molecule DTA2 with DMT spacer explored low value (Fig. 7). Additionally, the dyes with ETMN acceptor units and the DPT first π -spacer exhibited greater hyperpolarizability than others. Might be more electron-withdrawing groups fluoro (-F) on spacer and cyano (-CN) group on acceptor unit collectively created a robust pull-push architecture which stabilized the band gap between orbitals hence showed excellent results. This increase in the hyperpolarizability values might be due to the combined effect of powerful A units and the delocalized π -electrons that stabilize the molecule by lowering their orbitals bandgap and enhanced the polarizability. Overall, the decreasing order for β_{total} of all theoretically designed dyes was: DTA12 < DTA11 <

Table 1 Computed potential (IP), electron affinity (EA), electronegativity (X), global hardness (η), chemical potential (μ), global electrophilicity (ω) and global softness (σ) of investigated dyes(DTA1 -DTA12) obtained by DFT method using B3LYP/6-31G(d,p) level in a.u.

Compound	IP	EA	X	η	μ	ω	σ
JK-201	0.179	0.101	0.140	0.039	-0.140	0.250	12.775
DTA1	0.185	0.116	0.150	0.034	-0.150	0.326	14.424
DTA2	0.180	0.106	0.143	0.036	-0.143	0.278	13.573
DTA3	0.176	0.104	0.140	0.036	-0.140	0.271	13.781
DTA4	0.181	0.108	0.144	0.036	-0.144	0.285	13.70
DTA5	0.183	0.112	0.147	0.035	-0.147	0.306	14.090
DTA6	0.178	0.102	0.140	0.038	-0.140	0.258	13.151
DTA7	0.175	0.102	0.138	0.037	-0.138	0.261	13.613
DTA8	0.179	0.104	0.141	0.037	-0.141	0.268	13.411
DTA9	0.185	0.117	0.151	0.034	-0.151	0.339	14.778
DTA10	0.181	0.111	0.146	0.035	-0.146	0.306	14.376
DTA11	0.177	0.108	0.143	0.034	-0.143	0.296	14.476
DTA12	0.182	0.113	0.147	0.034	-0.147	0.315	14.526

Table 2 Computed transition maximum absorption wavelengths (λ_{max}), energy (E_{ge}/eV), oscillator strengths (f_{os}), transition moment ($\Delta\mu_{gm}$), light-harvesting efficiency (LHE) and transition natures of entitled compounds obtained by TD-DFT method using CAM-B3LYP/6-31G(d,p) level.

Dye	$E_{ge}(eV)$	$\lambda_{max}(nm)$	f_{os}	LHE	$\Delta\mu_{gm}$	MO transition
JK-201	2.7	484.7 (4 8 1) ^b	2.0	1	5.2	H →L (47%),H-1→L (41%)
DTA1	2.5	489.0	1.6	1	6.1	H-1→L (32%), H→L (52%)
DTA2	2.7	462.5	2.3	1	6.7	H-1→L (40%), H→L (32)
DTA3	2.5	493.1	2.1	1	5.6	H-1→L (32%), H→L (36%)
DTA4	2.5	492.7	2.2	1	5.1	H-1→L (31%), H→L (33%)
DTA5	2.4	513.6	2.3	1	3.8	H-1→L (46%), H→L (42%)
DTA6	2.5	504.8	2.9	1	4.9	H-1→L (51%), H→L (31%)
DTA7	2.3	533.1	2.7	1	5.0	H-1→L (40%), H→L (40%)
DTA8	2.4	527.6	2.8	1	4.5	H-1→L (42%), H→L (36%)
DTA-9	2.4	513.7	2.4	1	4.3	H-1→L (44%), H→L (44%)
DTA10	2.4	507.9	2.9	1	5.3	H-1→L (49%),H→L (32%)
DTA11	2.3	539.0	2.8	1	5.3	H-1→L (39%), H→L (41%)
DTA12	2.3	533.5	2.9	1	4.8	H-1→L (41%), H→L (38%)

H = HOMO, L = LUMO, H-1 = HOMO-1, etc.; Molecular orbitals = MO, b Experimental values in parentheses are from (Khan et al., 2019a).

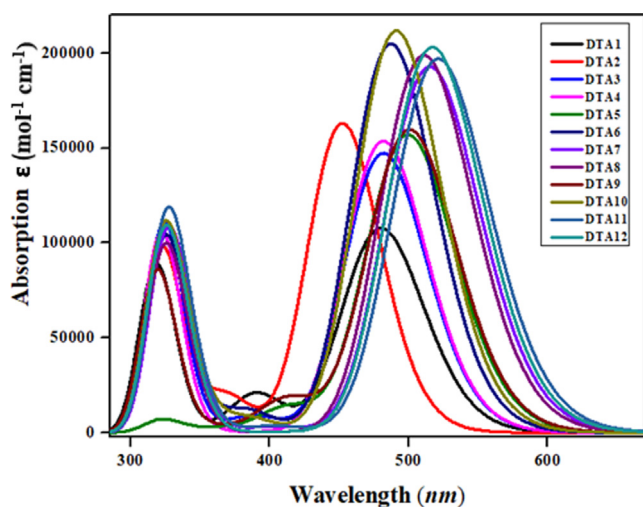


Fig. 5 Absorption spectra of entitled compounds (DTA1- DTA12) obtained by TD-DFT method using CAM-B3LYP/6-31G(d,p) level.

DTA10 < DTA9 < DTA8 < DTA7 < DTA4 < DTA-3 < DTA6 < DTA1 < DTA2 < DTA5.

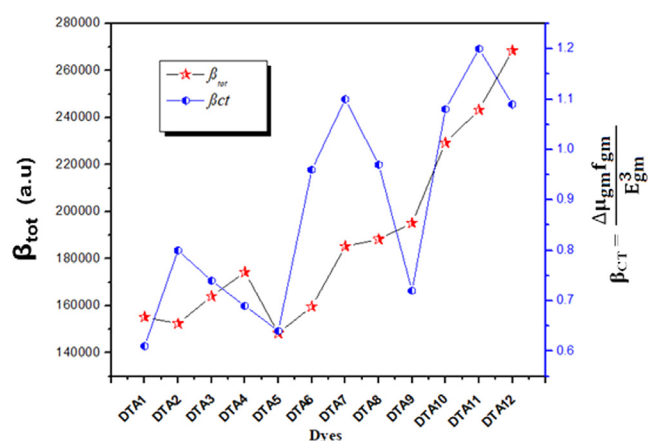
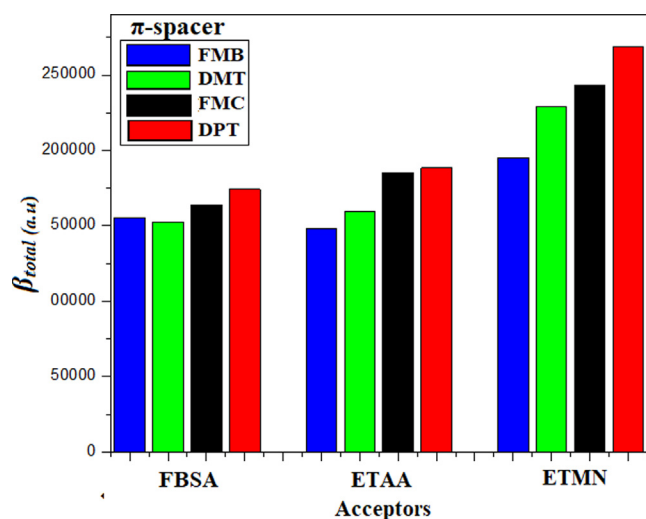
Additionally, hyperpolarizability findings of our designed dyes (DTA1-DTA12) were also compared with urea ($\beta_{total} = 43 a.u$), an organic reference compound (Kanis et al., 1994) and found considerably larger in entitled molecules. It was examined that in all investigated dyes from DTA1 to DTA12, β_{total} values were observed to be 3609, 3546, 3816, 4053, 3451, 3713, 4308, 4540, 5333, 5659, and 6244 times higher, respectively than urea.

4. Conclusions

A series of novel metal-free organic molecules (DTA1-DTA12) was theoretically designed from JK-201, a recently synthesized dye. The main object of this work was to elucidate the effect of various π -conjugated linkers and A units on the electronic, photophysical and NLO properties of DTA1-DTA12. DFT/ TD-DFT calculations indicated that π -spacers and acceptor

Table 3 Dipole polarizabilities and major contributing tensors (*a.u.*) of **DTA1** – **DTA12**.

Compounds	α_{xx}	α_{yy}	α_{zz}	$\langle \alpha \rangle$
DTA1	1563.94	751.57	504.16	939.89
DTA2	1809.66	846.34	435.09	1030.36
DTA3	1907.18	1037.53	607.03	1183.91
DTA4	1880.96	857.87	406.44	1048.42
DTA5	1936.09	747.39	553.80	2868.08
DTA6	2215.31	893.51	437.34	1182.05
DTA7	2353.53	1092.76	601.90	1349.39
DTA8	2317.13	879.34	436.48	1210.98
DTA9	2037.15	728.01	556.78	1107.31
DTA10	2359.95	877.84	435.79	1224.52
DTA11	2493.03	1092.78	587.55	1391.12
DTA12	2479.37	871.16	426.86	1259.13

**Fig. 6** Relationship between the β_{total} values and the corresponding $\Delta\mu_{gm}f_{gm}/E_{gm}^3$ values for investigated compounds (**DTA1**–**DTA12**).**Fig. 7** Graphical representation of hyperpolarizability of entitled chromophores.

units were auspicious groups for donor- π -acceptor architecture that excellently tuned the whole properties of derivatives. All species **DTA1**–**DTA12** exhibited a broader absorption spectrum in the visible region with reduced E_{ge} , higher oscillation strength, transition moment and LHE. The maximum bathochromic shift was expressed by **DTA11** dye ($\lambda_{max} = 539 \text{ nm}$). Further, the FMO study revealed all the designed compounds had a narrow bandgap (1.84–2.07 eV) than parent dye **JK-201** (2.13 eV). Additionally, GRP was also investigated, which disclosed that all the derivatives had minimum global hardness ($\eta = 0.034$ – 0.038 a.u.) and larger softness ($\sigma = 13.15$ – 14.77 a.u.) values showed that all the molecules were more reactive. The decreasing order of softness: **DTA9** > **DTA12** > **DTA11** > **DTA1** > **DTA10** > **DTA5** > **DTA3** > **DTA4** > **DTA2** > **DTA8** > **DTA6** > **JK-201**. Nonlinear optical investigation elucidated that all the investigated molecules have huge hyperpolarizability ($\beta_{total} = 148379.11$ – 268494.7074 a.u.). Among all the investigated dyes, the molecule **DTA5** has a larger value of the linear polarizability (4173.381 *a.u.*), while compound **DTA12** displayed a large β_{total} (268494.7074 *a.u.*). Nevertheless, β_{total} demonstrated broad agreement with $\Delta\mu_{gm}f_{gm}/E_{gm}^3$ values. So this present NLO compounds are considered an attractive domain for research. This computational work provides worthwhile insight for experimentalists to explore these attractive NLO materials for optics and electronics.

Declaration of Competing Interest

The authors declare that they have no known competing financial interests or personal relationships that could have appeared to influence the work reported in this paper.

Acknowledgments

The authors would like to express their gratitude to the Medical Key Subject Construction Project of Shanghai District, award Number (ZK2019B08), and the program of Minhang hospital, Fudan University hospital level project Number (2020MHJC07). Further, M. Imran and M. A. Assiri expressed appreciation to the Deanship of Scientific Research at King Khalid University Saudi Arabia for funding through

a research group program under grant number R.G.P. 1/297/42.

Appendix A. Supplementary material

Supplementary data to this article can be found online at <https://doi.org/10.1016/j.arabjc.2021.103295>.

References

- Ali, A. et al, 2020. Efficient Synthesis, SC-XRD, and Theoretical Studies of O-Benzene-sulfonylated Pyrimidines: Role of Noncovalent Interaction Influence in Their Supramolecular Network. *ACS Omega* 5, 15115–15128.
- Ali, 2021. Synthesis, Single-Crystal Exploration, and Theoretical Insights of Arylsulfonylated 2-Amino-6-methylpyrimidin Derivatives. *J. Mol. Struct.* 1243 (130789).
- Ans, M. et al, 2019. Development of fullerene free acceptors molecules for organic solar cells: A step way forward toward efficient organic solar cells. *Comput. Theor. Chem.* 1161, 26–38.
- Anthony, J.K. et al, 2008. Particle size-dependent giant nonlinear absorption in nanostructured Ni-Ti alloys. *Opt. Express* 16, 11193–11202.
- Breitung, E.M. et al, 2000. Thiazole and thiophene analogues of donor–acceptor stilbenes: molecular hyperpolarizabilities and structure–property relationships. *J. Am. Chem. Soc.* 122, 1154–1160.
- Chattaraj, P.K. et al, 2006. Electrophilicity Index. *Chem. Rev.* 106, 2065–2091.
- Chemla, D.S. (2012). *Nonlinear Optical Properties of Organic Molecules and Crystals VI, Vol 1* (Elsevier).
- Dai, X. et al, 2018. Unique D- π -A- π -D type fluorescent probes for the two-photon imaging of intracellular viscosity. *J. Mater. Chem. B* 6, 381–385.
- Eaton, D.F., 1991. *Nonlinear Optical Materials: The Great and Near Great*. In (ACS Publications).
- Ferdowsi, P. et al, 2018a. Molecular Design of Efficient Organic D-A–A Dye Featuring Triphenylamine as Donor Fragment for Application in Dye-Sensitized Solar Cells. *ChemSusChem* 11, 494–502.
- Ferdowsi, P. et al, 2018b. Molecular Design of Efficient Organic D-A–A Dye Featuring Triphenylamine as Donor Fragment for Application in Dye-Sensitized Solar Cells. *ChemSusChem* 11, 494–502.
- Frisch, M., et al., 2009. D. 0109, Revision D. 01. Gaussian, Inc Wallingford.
- Frisch, M., et al., 2009, Gaussian, Inc., Wallingford CT. Gaussian 09.
- Fukui, K., 1982. Role of Frontier Orbitals in Chemical Reactions. *Science* 218, 747.
- Hanwell, M.D. et al, 2012. Avogadro: an advanced semantic chemical editor, visualization, and analysis platform. *J. Cheminf.* 4, 1–17.
- Haroon, M. et al, 2017. An Interesting Behavior and Nonlinear Optical (NLO) Response of Hexamolybdate Metal Cluster: Theoretical Insight into Electro-Optic Modulation of Hybrid Composites. *J. Cluster Sci.* 28, 2693–2708.
- Hochberg, M. et al, 2006. Terahertz all-optical modulation in a silicon–polymer hybrid system. *Nat. Mater.* 5, 703–709.
- Iliopoulos, K. et al, 2010. Physical origin of the third order nonlinear optical response of orthogonal pyrrolo-tetrathiafulvalene derivatives. *Appl. Phys. Lett.* 97, 101104.
- Ivanov, I.P. et al, 2013. Nonlinear absorption properties of the charge states of nitrogen-vacancy centers in nanodiamonds. *Opt. Lett.* 38, 1358–1360.
- Janjua, M.R.S.A., 2012. Quantum mechanical design of efficient second-order nonlinear optical materials based on heteroaromatic imido-substituted hexamolybdates: First theoretical framework of POM-based heterocyclic aromatic rings. *Inorg. Chem.* 51, 11306–11314.
- Janjua, M.R.S.A. et al, 2014a. Quantum chemical perspective of efficient NLO materials based on dipolar trans-tetraammineruthenium (II) complexes with pyridinium and thiocyanate ligands: First theoretical framework. *Comput. Theor. Chem.* 1033, 6–13.
- Janjua, M.R.S.A. et al, 2015a. Solvent-Dependent Non-Linear Optical Properties of 5,5'-Disubstituted-2,2'-bipyridine Complexes of Ruthenium(II): A Quantum Chemical Perspective. *Aust. J. Chem.* 68.
- Janjua, M.R.S.A. et al, 2015b. Solvent-Dependent Non-Linear Optical Properties of 5, 5'-Disubstituted-2, 2'-bipyridine Complexes of Ruthenium (ii): A Quantum Chemical Perspective. *Aust. J. Chem.* 68, 1502–1507.
- Janjua, M.R.S.A. et al, 2014b. Electronic absorption spectra and nonlinear optical properties of ruthenium acetylide complexes: a DFT study toward the designing of new high NLO response compounds. *Acta Chim. Slov.* 61.
- Janjua, M.R.S.A. et al, 2010. Tuning Second-Order Non-linear (NLO) Optical Response of Organoimido-Substituted Hexamolybdates through Halogens: Quantum Design of Novel Organic-Inorganic Hybrid NLO Materials. *Aust. J. Chem.* 63, 836–844.
- Janjua, M.R.S.A. et al, 2016. First principle study of electronic and non-linear optical (NLO) properties of triphenylamine dyes: interactive design computation of new NLO compounds. *Aust. J. Chem.* 69, 467–472.
- Kanis, D.R. et al, 1994. Design and construction of molecular assemblies with large second-order optical nonlinearities. *Quant. Chem. Asp. Chem. Rev.* 94, 195–242.
- Kasap, S., Capper, P., 2017. *Springer handbook of electronic and photonic materials*. Springer.
- Khalid, M. et al, 2020. First principles study of electronic and nonlinear optical properties of A-D- π -A and D-A-D- π -A configured compounds containing novel quinoline–carbazole derivatives. *RSC Adv.* 10, 22273–22283.
- Khalid, M. et al, 2020b. Exploration of Noncovalent Interactions, Chemical Reactivity, and Nonlinear Optical Properties of Piperidone Derivatives: A Concise Theoretical Approach. *ACS Omega* 5, 13236–13249.
- Khalid, M. et al, 2020c. An efficient synthesis, structural (SC-XRD) and spectroscopic (FTIR, ¹HNMR, MS spectroscopic) characterization of novel benzofuran-based hydrazones: An experimental and theoretical studies. *J. Mol. Struct.* 1216, 128318.
- Khan, M.U. et al, 2019a. Prediction of second-order nonlinear optical properties of D- π -A compounds containing novel fluorene derivatives: a promising route to giant hyperpolarizabilities. *J. Cluster Sci.* 30, 415–430.
- Khan, M.U. et al, 2019b. Quantum chemical designing of indolo[3,2,1-jk]carbazole-based dyes for highly efficient nonlinear optical properties. *Chem. Phys. Lett.* 719, 59–66.
- Khan, M.U. et al, 2018. First theoretical framework of triphenylamine–dicyanovinylene-based nonlinear optical dyes: structural modification of π -linkers. *J. Phys. Chem. C* 122, 4009–4018.
- Khoo, I.C., 2014. Nonlinear optics, active plasmonics and metamaterials with liquid crystals. *Prog. Quant. Electron.* 38, 77–117.
- Kilper, D.C., 2010. Chapter 11 - Optical performance monitoring based on nonlinear optical techniques. In: Chan, C.C.K. (Ed.), *Optical Performance Monitoring*. Academic Press, Oxford, pp. 301–317.
- Kulyk, B. et al, 2017. Functionalized azo-based iminopyridine rhenium complexes for nonlinear optical performance. *Dyes Pigm.* 145, 256–262.
- Lacroix, P.G. et al, 1994. Stilbazolium-MPS ₃ Nanocomposites with Large Second-Order Optical Nonlinearity and Permanent Magnetization. *Science* 263, 658.
- Lesar, A., Milošev, I., 2009. Density functional study of the corrosion inhibition properties of 1,2,4-triazole and its amino derivatives. *Chem. Phys. Lett.* 483, 198–203.

- Long, G. et al, 2014. Impact of the Electron-Transport Layer on the Performance of Solution-Processed Small-Molecule Organic Solar Cells. *ChemSusChem* 7, 2358–2364.
- Manzoni, M.T. et al, 2015. Second-order quantum nonlinear optical processes in single graphene nanostructures and arrays. *New J. Phys.* 17, 083031.
- Mohankumar, V. et al, 2015. Computational Studies on 5-(4-(4-(Diphenylamino)Phenylamino)phenyl)-2-Cyanopenta-2,4-enoic Acid for dye Sensitized Solar cell Application. *Mater. Today: Proc.* 2, 1041–1045.
- Nagarajan, B. et al, 2017. Novel ethynyl-pyrene substituted phenothiazine based metal free organic dyes in DSSC with 12% conversion efficiency. *J. Mater. Chem. A* 5, 10289–10300.
- Oudar, J.L., Chemla, D.S., 1977. Hyperpolarizabilities of the nitroanilines and their relations to the excited state dipole moment. *J. Chem. Phys.* 66, 2664–2668.
- Paek, S. et al, 2010. Molecular engineering of efficient organic sensitizers incorporating a binary π -conjugated linker unit for dye-sensitized solar cells. *J. Phys. Chem. C* 114, 14646–14653.
- Parr, R.G. et al, 1978. Electronegativity: The density functional viewpoint. *J. Chem. Phys.* 68, 3801–3807.
- Parr, R.G. et al, 1999. Electrophilicity Index. *J. Am. Chem. Soc.* 121, 1922–1924.
- Peng, Z., Yu, L., 1994. Second-order nonlinear optical polyimide with high-temperature stability. *Macromolecules* 27, 2638–2640.
- Qin, C., Clark, A.E., 2007. DFT characterization of the optical and redox properties of natural pigments relevant to dye-sensitized solar cells. *Chem. Phys. Lett.* 438, 26–30.
- Roncali, J., 2009. Molecular Bulk Heterojunctions: An Emerging Approach to Organic Solar Cells. *Acc. Chem. Res.* 42, 1719–1730.
- Spiridon, M.C. et al, 2015. Novel pendant azobenzene/polymer systems for second harmonic generation and optical data storage. *Dyes Pigm.* 114, 24–32.
- Sung, P.-H., Hsu, T.-F., 1998. Thermal stability of NLO sol-gel networks with reactive chromophores. *Polymer* 39, 1453–1459.
- Tsutsumi, N. et al, 1998. Nonlinear optical (NLO) polymers. 3. NLO polyimide with dipole moments aligned transverse to the imide linkage. *Macromolecules* 31, 7764–7769.
- Wu, S. et al, 2012. Quantum-Enhanced Tunable Second-Order Optical Nonlinearity in Bilayer Graphene. *Nano Lett.* 12, 2032–2036.
- Xie, R.H., 2001. Chapter 6 - Nonlinear optical properties of fullerenes and carbon nanotubes. In: Singh Nalwa, H. (Ed.), *Handbook of Advanced Electronic and Photonic Materials and Devices*. Academic Press, Burlington, pp. 267–307.
- Yamada, S. et al, 2018. Color tuning donor-acceptor-type azobenzene dyes by controlling the molecular geometry of the donor moiety. *Dyes Pigm.* 150, 89–96.
- Yamashita, S., 2011. A tutorial on nonlinear photonic applications of carbon nanotube and graphene. *J. Lightwave Technol.* 30, 427–447.
- Yanai, T. et al, 2004. A new hybrid exchange-correlation functional using the Coulomb-attenuating method (CAM-B3LYP). *Chem. Phys. Lett.* 393, 51–57.
- Zhurko, G., Zhurko, D., 2009. ChemCraft, version 1.6. URL: <http://www.chemcraftprog.com>.
- Zyss, J., Ledoux, I., 1994. Nonlinear optics in multipolar media: theory and experiments. *Chem. Rev.* 94, 77–105.